arXiv:1104.3285v3 [gr-qc] 24 Aug 2011

Fine structure of high-energy absorption cross sections for black holes

Yves Décanini

Equipe Physique Théorique, SPE, UMR 6134 du CNRS et de l'Université de Corse, Université de Corse, Faculté des Sciences, BP 52, F-20250 Corte, France

Antoine Folacci

Equipe Physique Théorique, SPE, UMR 6134 du CNRS et de l'Université de Corse, Université de Corse, Faculté des Sciences, BP 52, F-20250 Corte, France
and
Centre de Physique Théorique, UMR 6207 du CNRS et des Universités Aix-Marseille 1 et 2 et de l'Université du Sud Toulon-Var, CNRS-Luminy Case 907, F-13288 Marseille, France

Bernard Raffaelli

Equipe Physique Théorique, SPE, UMR 6134 du CNRS et de l'Université de Corse, Université de Corse, Faculté des Sciences, BP 52, F-20250 Corte, France

E-mail: `decanini@univ-corse.fr` and `folacci@univ-corse.fr` and `raffaelli@univ-corse.fr`

Abstract.
The high-energy absorption cross section of the Schwarzschild black hole is well approximated, in the eikonal regime, by the sum of two terms: the geometrical cross section of the black hole photon sphere and the contribution of a sinc function involving the geometrical characteristics (orbital period and Lyapunov exponent) of the null unstable geodesics lying on this photon sphere. From a numerical analysis, we show that, beyond the eikonal description, this absorption cross section presents a simple fine structure. We then describe it analytically by using Regge pole techniques and interpret it in geometrical terms. We naturally extend our analysis to arbitrary static spherically symmetric black holes endowed with a photon sphere and we then apply our formalism to Schwarzschild-Tangherlini and Reissner-Nordström black holes. Finally, on the example of the Schwarzschild black hole, we show numerically that a complicated hyperfine structure lying beyond the fine structure can also be observed.

PACS numbers: 04.70.-s, 04.50.Gh

1. Introduction

In a recent paper [1], by using Regge pole techniques, we have developed a new and universal description of the absorption problem for a massless scalar field propagating in static spherically symmetric black holes of arbitrary dimension endowed with a photon sphere. We have shown, in particular, that the high-energy absorption cross section is well approximated, in the eikonal regime, by the sum of two contributions:

the geometrical cross section of the black hole photon sphere (i.e., the so-called capture cross section of the black hole) and a sinc function involving the geometrical characteristics (orbital period and Lyapunov exponent) of the null unstable geodesics lying on this photon sphere. We have therefore provided a rigorous analysis as well as a clear physical description of a result well known in black hole physics (see, e.g., Refs. [2, 3, 4, 5, 6, 7, 8, 9, 10]), the fact that in general, at high energies, the absorption cross section of a black hole oscillates around a limiting constant value, explaining within the same formalism the existence of this limiting value and of the fluctuations.

In this paper, from the complex angular momentum formalism already developed in Ref. [1] and by using new asymptotic expansions for the residues of the "greybody" factors, we shall go beyond the eikonal description of the high-energy absorption cross section for black holes. More precisely, in section 2, from a numerical analysis, we shall first show that, beyond the eikonal description, the absorption cross section of the Schwarzschild black hole presents a simple fine structure. We shall then describe it analytically and interpret it in geometrical terms. In section 3, we shall extend the previous considerations to static spherically symmetric black holes endowed with a photon sphere and apply the formalism developed to the five- and six-dimensional Schwarzschild-Tangherlini black holes and to the four-dimensional Reissner-Nordström black hole. In a brief conclusion (our section 4), we shall consider some possible consequences of our present work and show numerically, for the Schwarzschild black hole, the existence of a complicated hyperfine structure lying beyond the fine structure. Finally, in a much more technical appendix, we shall provide some asymptotic expansions for the Regge poles and for the corresponding residues of the greybody factors which are useful to describe analytically the fine structure and which could be helpful to analyze the hyperfine structure.

Throughout this paper, we shall use units such that $\hbar = c = G = 1$ and we shall assume a harmonic time dependence $\exp(-i\omega t)$ for the fields.

2. Fine structure of the high-energy absorption cross sections of the Schwarzschild black hole

We begin by various considerations relative to (i) the Schwarzschild black hole and (ii) a scalar field theory defined on this gravitational background that we shall use extensively in this section and in subsection A.1 of the appendix. This moreover permits us to establish all our notations:

(i) We first recall that the exterior of the Schwarzschild black hole of mass M is usually defined as the manifold $\mathcal{M} =]-\infty, +\infty[_t \times]2M, +\infty[_r \times S^2$ with metric $ds^2 = -f(r)dt^2 + f(r)^{-1}dr^2 + r^2 d\sigma_2^2$. Here $d\sigma_2^2$ denotes the metric on the unit 2-sphere S^2 and $f(r) = (1 - 2M/r)$. We remark that, instead of the standard radial Schwarzschild coordinate r, it is sometimes more convenient to use the so-called tortoise coordinate $r_*(r)$ defined by $dr/dr_* = f(r)$ which provides a bijection from $]2M, +\infty[$ to $]-\infty, +\infty[$. We also note that this black hole has a photon sphere located at $r = 3M \equiv r_c$, that the corresponding critical impact parameter is given by $b_c = 3\sqrt{3}M$ (see, e.g., Chap. 25 of Ref. [11]) and that, as a consequence, the geometrical cross section of this black hole is $\sigma_{\rm geo} = \pi b_c^2 = 27\pi M^2$.

(ii) We also recall that the wave equation for a massless scalar field propagating on the Schwarzschild black hole reduces, after separation of variables and

the introduction of the radial partial wave functions $\phi_{\omega\ell}(r)$, to the Regge-Wheeler equation

$$\frac{d^2\phi_{\omega\ell}}{dr_*^2} + \left[\omega^2 - V_\ell(r_*)\right]\phi_{\omega\ell} = 0 \tag{2.1}$$

where the so-called Regge-Wheeler potential $V_\ell(r_*)$ is given in terms of the radial Schwarzschild coordinate by

$$V_\ell(r) = \left(\frac{r-2M}{r}\right)\left[\frac{(\ell+1/2)^2-1/4}{r^2} + \frac{2M}{r^3}\right]. \tag{2.2}$$

Here $\omega > 0$ denotes the frequency of the mode-solution considered while $\ell \in \mathbb{N}$ is the ordinary angular momentum index. We note that for ω and ℓ given, the radial amplitude $\phi_{\omega\ell}(r_*)$ moreover satisfies the boundary conditions

$$\phi_{\omega\ell}(r_*) \sim \begin{cases} T_\ell(\omega)e^{-i\omega r_*} & \text{for } \ r_* \to -\infty, \\ \\ e^{-i\omega r_*} + R_\ell(\omega)e^{+i\omega r_*} & \text{for } \ r_* \to +\infty, \end{cases} \tag{2.3}$$

where $T_\ell(\omega)$ and $R_\ell(\omega)$ are transmission and reflection coefficients. We finally recall that the greybody factors (the absorption probabilities for particles with energy ω and angular momentum ℓ) are given by

$$\Gamma_\ell(\omega) = |T_\ell(\omega)|^2 \tag{2.4}$$

and that, for the massless scalar field considered here, the black hole absorption cross section can be expressed in terms of the greybody factors in the form

$$\sigma_{\text{abs}}(\omega) = \frac{\pi}{\omega^2}\sum_{\ell=0}^{+\infty}(2\ell+1)\Gamma_\ell(\omega). \tag{2.5}$$

It should be noted that the series (2.5) can be evaluated with a very great precision by solving numerically the problem defined by (2.1), (2.2) and (2.3) but that its evaluation is very time consuming for high frequencies.

In Ref. [1], by using Regge pole techniques, we have proved that the high-energy behavior of the absorption cross section of the Schwarzschild black hole (2.5) is well approximated, in the eikonal regime, by the sum of two terms (what we shall call from now on the eikonal description): the geometrical cross section of the black hole photon sphere and a sinc function involving the geometrical characteristics (orbital period and Lyapunov exponent) of the null unstable geodesics lying on this photon sphere (see also Ref. [2] for a fit of the absorption cross section of the Schwarzschild black hole involving a sinc function but based mainly on numerical considerations). More precisely, we have rigorously shown that the fluctuations of (2.5) around the geometrical cross section σ_{geo} are well described by the very simple formula

$$\sigma_{\text{abs}}^{\text{osc}}(\omega) = -8\pi\, e^{-\pi}\, \sigma_{\text{geo}}\, \text{sinc}\left[2\pi(3\sqrt{3}M)\omega\right], \tag{2.6}$$

where $\text{sinc}\, x \equiv (\sin x)/x$ is the sine cardinal. Let us note that the argument of the sinc involves the orbital period, $2\pi(3\sqrt{3}M) = 2\pi b_c$, of a massless particle orbiting the black hole on the photon sphere [12, 13, 14, 15] while the coefficient $8\pi e^{-\pi}$ is linked to the Lyapunov exponent of the geodesic followed by the particle (see Refs. [1, 14, 15] for more precisions on this last point). This formula permits us to interpret naturally the period of the maxima (or the minima, or the zeros) of the fluctuations in terms of

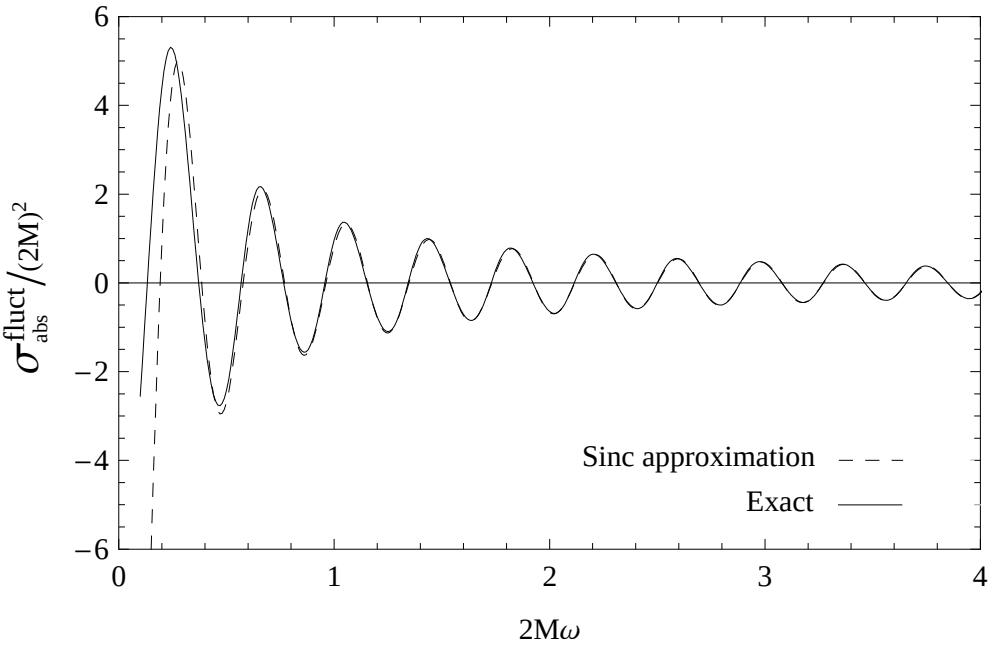

Figure 1. Fluctuations of the total absorption cross section, $\sigma_{\rm abs}^{\rm fluct} \equiv \sigma_{\rm abs} - \sigma_{\rm geo}$, for a massless scalar field propagating in the Schwarzschild geometry. The exact curve is obtained numerically from (2.5) while the sinc approximation is given by (2.6).

constructive interferences of the "surface waves" trapped near the photon sphere (see also Refs. [12] and [13] for related aspects).

The agreement of (2.6) with the exact result obtained numerically from (2.5) is very good, even for low frequencies (see figure 1). However, if we consider the difference between the two curves displayed, i.e., if we consider the behavior of the function

$$\Delta\sigma_{\rm abs}^{\rm fluct,\,fine}(\omega) \equiv \sigma_{\rm abs}(\omega) - [\sigma_{\rm geo} + \sigma_{\rm abs}^{\rm osc}(\omega)]\,, \tag{2.7}$$

we show that beyond the eikonal description, the absorption cross section presents a simple fine structure (see figure 2). Because the amplitude of this fine structure is around $5-10\,\%$ of that of the eikonal fluctuations, its existence must be mentioned and could even have interesting physical consequences. So it seems to us worthwhile to describe it mathematically.

With this aim in mind, let us first recall how we obtained the eikonal description of the absorption cross section (2.5). In Ref. [1], from the Regge pole machinery, we have shown that (2.5) can be replaced by the series

$$\sigma_{\rm abs}(\omega) = 27\pi M^2 - \frac{4\pi^2}{\omega^2}\,{\rm Re}\left(\sum_{n=1}^{+\infty}\frac{e^{i\pi[\lambda_n(\omega)-1/2]}\,\lambda_n(\omega)\gamma_n(\omega)}{\sin[\pi(\lambda_n(\omega)-1/2)]}\right) + \underset{M\omega\to+\infty}{\mathcal{O}}\left(\frac{1}{(M\omega)^2}\right). \tag{2.8}$$

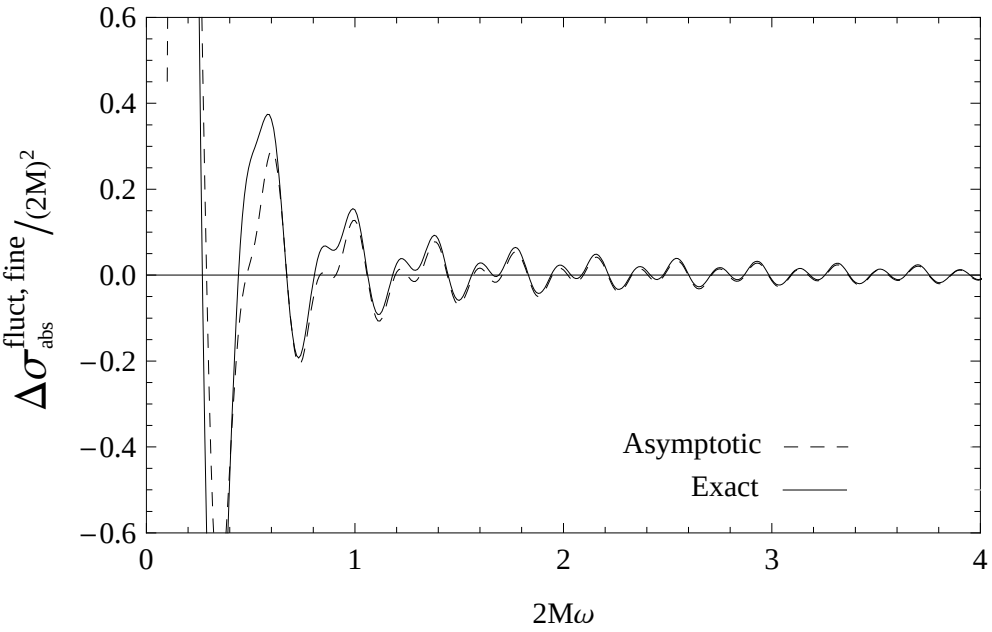

Figure 2. Fine structure of the total absorption cross section, $\Delta\sigma_{\rm abs}^{\rm fluct,\,fine}(\omega) \equiv \sigma_{\rm abs}(\omega) - \left[\sigma_{\rm geo} + \sigma_{\rm abs}^{\rm osc}(\omega)\right]$, for a massless scalar field propagating in the Schwarzschild geometry. The exact curve is obtained numerically from (2.5) and (2.6) while the asymptotic result is given by (2.12).

In equation (2.8), the $\lambda_n(\omega)$ with $n \in \mathbb{N} \setminus \{0\}$ are those of the (Regge) poles of the analytic extension $\Gamma_{\lambda-1/2}(\omega)$ of the greybody factor $\Gamma_\ell(\omega)$ lying in the first quadrant of the complex λ plane and the $\gamma_n(\omega)$ are the associated residues. It is important to recall that (2.8) converges very rapidly and that the contribution of the Regge poles with $n > 1$ is practically negligible (see figure 2 of Ref. [1]). So, by using the rough approximations

$$\lambda_n(\omega) = 3\sqrt{3}M\omega + i\,(n - 1/2) + \underset{M\omega\to+\infty}{\mathcal{O}}\left(\frac{1}{M\omega}\right) \tag{2.9}$$

and

$$\gamma_n(\omega) = -\frac{1}{2\pi} + \underset{M\omega\to+\infty}{\mathcal{O}}\left(\frac{1}{M\omega}\right), \tag{2.10}$$

and taking into account only the contribution of the first Regge pole, we obtained from (2.8) the eikonal approximation (2.6) for the fluctuations of the absorption cross section (2.5).

Of course, approximations (2.9) and (2.10) are too rough to permit us to understand the existence of the fine structure. But if we now consider the asymptotic expansions (A.13) and (A.14) with $n = 1$ and $s = 0$, by using the relation (for $a \in \mathbb{R}$)

$$\frac{e^{i\pi(z-a)}}{\sin[\pi(z-a)]} = -2i\sum_{m=1}^{+\infty} e^{i2m\pi(z-a)} \quad \text{valid if Im } z > 0, \tag{2.11}$$

we can show from (2.8) that (2.5) can be approximated by

$$\sigma_{\rm abs}(\omega) \approx \sigma_{\rm geo}\left(1-8\pi\, e^{-\pi}\,\frac{\sin\left[2\pi(3\sqrt{3}M)\omega\right]}{2\pi(3\sqrt{3}M)\omega}\right.$$
$$\left.+16\pi e^{-2\pi}\frac{\sin\left[4\pi(3\sqrt{3}M)\omega\right]}{4\pi(3\sqrt{3}M)\omega}+\frac{4\pi^2e^{-\pi}(-39+7\pi)}{27}\frac{\cos\left[2\pi(3\sqrt{3}M)\omega\right]}{[2\pi(3\sqrt{3}M)\omega]^2}\right). \quad (2.12)$$

In (2.12), the first two terms correspond to the eikonal description constructed in Ref. [1] while the third and fourth ones describe the fine structure of the absorption cross section. In figure 2 we have compared the exact fine structure numerically evaluated with the result provided by the third and fourth terms of (2.12). The agreement is truly remarkable. In fact, the error made on the exact absorption cross section (2.5) or on its fluctuations around $\sigma_{\rm geo}$ is considerably reduced by using (2.12) (see also figure 3 and the associated comment in section 4).

It is now important, from a physical point of view, to note that the fine structure, as the eikonal contribution, is only due to the "surface wave" trapped near the photon sphere which is associated with the first Regge pole (for the interpretation of Regge poles in terms of "surface waves", we refer to Refs. [16, 12, 13, 14]. However, in order to describe the fine structure, we must now take into account (i) the multiple circumnavigations around the black hole of this surface wave (the "beats" in the fine structure observed in figure 2 are due to interferences between terms involving the orbital period of a massless particle orbiting the black hole on the photon sphere and its second harmonic) and (ii) its dispersive character (the amplitude of the first harmonic contribution is constructed, in part, from the nonlinearities of the first Regge pole trajectory, i.e., comes from the term in $1/(M\omega)$ of (A.13)).

To conclude this section, we would like to remark that with equation (2.12) we have at our disposal a rather simple and very accurate approximation permitting us to describe qualitatively and quantitatively the high-energy behavior of the absorption cross section of the Schwarzschild black hole and to thus avoid very time-consuming calculations. It is moreover interesting to note that, for "very high energies", only the first three terms of (2.12) must be taken into account what simplifies considerably this approximation due to the elimination of a rather inelegant term.

3. Fine structure of high-energy absorption cross sections for static spherically symmetric black holes

3.1. General theory

The analysis developed in the previous section can be naturally extended to the more general case of a massless scalar field theory defined on a static spherically symmetric black hole of arbitrary dimension $d \geq 4$ endowed with a photon sphere. The exterior of such a black hole can be defined as the manifold $\mathcal{M} =]-\infty, +\infty[_t \times]r_h, +\infty[_r \times S^{d-2}$ with metric $ds^2 = -f(r)dt^2 + f(r)^{-1}dr^2 + r^2 d\sigma^2_{d-2}$ where $d\sigma^2_{d-2}$ denotes the metric on the unit $(d-2)$-sphere S^{d-2}. Here the (standard) coordinate r_h of the event horizon is assumed to be a simple root of $f(r)$. We furthermore assume that we have $f(r) > 0$ for $r > r_h$ and $\lim_{r\to+\infty} f(r) = 1$. In other words, the gravitational background considered is an asymptotically flat one and the tortoise coordinate $r_*(r)$

defined again by $dr/dr_* = f(r)$ provides a bijection from $]r_h, +\infty[$ to $]-\infty, +\infty[$. The existence of a photon sphere located at $r_c \in]r_h, +\infty[$ is ensured if we finally assume that the conditions $f'(r_c) - (2/r_c)f(r_c) = 0$ and $f''(r_c) - (2/r_c^2)f(r_c) < 0$ are satisfied (see Ref. [14] for more details on these last assumptions). It should be also noted that, for such a black hole, the critical impact parameter and the corresponding geometrical cross section are now given respectively by $b_c = r_c/\sqrt{f(r_c)}$ and $\sigma_{\rm geo} = \pi^{(d-2)/2} b_c^{d-2}/\Gamma(d/2)$ (see, e.g., Ref. [3]). Of course, when $f(r) = 1 - 2M/r$ and $d = 4$ we recover all the results concerning the Schwarzschild black hole we have listed at the beginning of section 2.

In order to simplify various expressions appearing in this section and in subsection A.2 of the appendix, we introduce the following notations:

$$f_c \equiv f(r_c) \quad \text{and} \quad f_c^{(p)} \equiv f^{(p)}(r_c) \quad \text{for} \quad p \geq 1 \tag{3.1}$$

and

$$\eta_c \equiv \frac{1}{2}\sqrt{4 f_c - 2 r_c^2 f_c^{(2)}}. \tag{3.2}$$

As already noted and discussed in Ref. [14], the η_c parameter represents a kind of measure of the instability of the circular orbits lying on the photon sphere and can be expressed in terms of the Lyapunov exponent corresponding to these orbits introduced in Ref. [15].

The wave equation for a massless scalar field propagating on this gravitational background still reduces, after separation of variables and the introduction of the radial partial wave functions $\phi_{\omega\ell}(r)$ with $\omega > 0$ and $\ell \in \mathbb{N}$, to the Regge-Wheeler equation (2.1) but, instead of (2.2), we have

$$V_\ell(r) = f(r) \left[\frac{[\ell + (d-3)/2]^2 - [(d-3)/2]^2}{r^2} + \frac{(d-2)(d-4)}{4r^2} f(r) + \left(\frac{d-2}{2r}\right) f'(r) \right]. \tag{3.3}$$

The boundary conditions (2.3) remain valid and the greybody factors are still defined by (2.4) but, now, the black hole absorption cross section is given by (see Ref. [17])

$$\sigma_{\rm abs}(\omega) = \frac{\pi^{(d-2)/2}}{\Gamma\left[(d-2)/2\right] \omega^{d-2}} \sum_{\ell=0}^{+\infty} \frac{(\ell + d - 4)!}{\ell!} \left(2\ell + d - 3\right) \Gamma_\ell(\omega). \tag{3.4}$$

In Ref. [1] we have shown that the fluctuations of (3.4) around the geometrical cross section are described by the Regge pole series

$$\sigma_{\rm abs}^{\rm RP}(\omega) = -\frac{4\pi^{d/2}}{\Gamma\left[(d-2)/2\right] \omega^{d-2}} \, {\rm Re} \left(\sum_{n=1}^{+\infty} \frac{\Gamma[\lambda_n(\omega) + (d-3)/2]}{\Gamma[\lambda_n(\omega) - (d-5)/2]} \frac{e^{i\pi[\lambda_n(\omega) - (d-3)/2]} \lambda_n(\omega) \gamma_n(\omega)}{\sin[\pi(\lambda_n(\omega) - (d-3)/2)]} \right). \tag{3.5}$$

Of course, at first sight such a series, even if it provides an exact description of the fluctuations, does not seem really interesting from a physical point of view. In Ref. [1], we have been able to extract from it an eikonal approximation of the absorption cross section based on rough approximations for the Regge poles and their

residues. In subsection A.2 of the appendix, we have obtained one more order for these approximations so we can now go beyond the eikonal description and construct the fine structure of the absorption cross section. By using the asymptotic expansions (A.18) and (A.20) for the Regge poles $\lambda_n(\omega)$ and the residues $\gamma_n(\omega)$, as well as (2.11) and

$$\frac{\Gamma(z+a)}{\Gamma(z+b)} \sim \left(\frac{1}{z}\right)^{-a+b} \qquad \text{valid if } |z| \to +\infty \text{ and } |\arg z| < \pi, \tag{3.6}$$

and keeping only the contribution of the first Regge pole in (3.5), we obtain

$$\begin{aligned}\sigma_{\text{abs}}(\omega) \approx \sigma_{\text{geo}} \Bigg(& 1 + (-1)^{d-3}\, 4(d-2)\pi\, \eta_c\, e^{-\pi\eta_c} \frac{\sin\left[2\pi(r_c/\sqrt{f_c})\omega\right]}{2\pi(r_c/\sqrt{f_c})\omega} \\ & + 8(d-2)\pi\eta_c e^{-2\pi\eta_c} \frac{\sin\left[4\pi(r_c/\sqrt{f_c})\omega\right]}{4\pi(r_c/\sqrt{f_c})\omega} \\ & - (-1)^{d-3} 4(d-2)\pi^2 e^{-\pi\eta_c} \left[a_c - (d-3)\eta_c^2 - 2\pi\eta_c a_1\right] \frac{\cos\left[2\pi(r_c/\sqrt{f_c})\omega\right]}{[2\pi(r_c/\sqrt{f_c})\omega]^2} \\ & - 16(d-2)\pi^2 e^{-2\pi\eta_c} \left[a_c - (d-3)\eta_c^2 - 4\pi\eta_c a_1\right] \frac{\cos\left[4\pi(r_c/\sqrt{f_c})\omega\right]}{[4\pi(r_c/\sqrt{f_c})\omega]^2} \Bigg). \end{aligned} \tag{3.7}$$

In (3.7), the first two terms correspond to the eikonal description constructed in section 4 of Ref. [1] while the third, fourth and fifth ones describe the fine structure of the absorption cross section. Let us note that the arguments of the sine and cosine functions involve the orbital period, $2\pi(r_c/\sqrt{f_c}) = 2\pi b_c$, of a massless particle orbiting the black hole on the photon sphere as well as its second harmonic. Of course, equation (3.7) generalizes (2.12) for static spherically symmetric black holes and, *mutatis mutandis*, the physical interpretation of the fine structure for the Schwarzschild black hole provided in section 2 remains valid in the general case. The coefficients a_c and a_1 which appear in the last two terms of (3.7) are defined in the appendix (see equation (A.21) for a_c and equation (A.19) with $n = 1$ for a_1) and are expressed in terms of the derivatives of $f(r)$ taken on the photon sphere. It is also important to note that the fifth term of (3.7) was not present for the Schwarzschild black hole. In fact, we have discarded it in section 2 because it was numerically negligible for this particular black hole. As we shall see later, it is also numerically insignificant for the five- and six-dimensional Schwarzschild-Tangherlini black holes and for the four-dimensional Reissner-Nordström black hole. However, we consider that, in the general case, it cannot be discarded.

To conclude the general theory, let us remark that for "very high frequencies", we can eliminate the last two terms of (3.7) and we have therefore at our disposal a nice and simple formula describing accurately the absorption cross section for a massless scalar field propagating on an arbitrary static and spherically symmetric black hole.

3.2. Application 1: Schwarzschild-Tangherlini black holes

We now apply the general theory developed in the previous subsection to Schwarzschild-Tangherlini black holes. They are generalization of the four-dimensional Schwarzschild black hole constructed in the sixties by Tangherlini [18]. For a d-dimensional Schwarzschild-Tangherlini black hole, we have

$$f(r) = 1 - \left(\frac{r_h}{r}\right)^{d-3}. \tag{3.8}$$

Here r_h, which denotes the standard coordinate of the event horizon, is linked to the mass M of the black hole by

$$r_h^{d-3} = \frac{16\pi M}{(d-2)\mathcal{A}_{d-2}} \tag{3.9}$$

where $\mathcal{A}_{d-2} = 2\pi^{(d-1)/2}/\Gamma[(d-1)/2]$ is the area of the unit sphere S^{d-2}. The photon sphere is then located at

$$r_c = r_h \left(\frac{d-1}{2}\right)^{1/(d-3)}, \tag{3.10a}$$

the associated η_c parameter is given by

$$\eta_c = \sqrt{d-3} \tag{3.10b}$$

while the corresponding critical impact parameter $b_c = r_c/\sqrt{f_c}$ reads

$$b_c = \sqrt{\frac{d-1}{d-3}} r_c. \tag{3.10c}$$

For $d = 5$, we have $\sigma_{\rm geo} = (4\pi/3)b_c^3$ with $b_c = \sqrt{2}r_c$ and $r_c = \sqrt{2}r_h$ as well as $\eta_c = \sqrt{2}$ and the general formula (3.7) then reduces to

$$\sigma_{\rm abs}^{\rm ST\,d=5}(\omega) \approx \sigma_{\rm geo}\left(1 + 12\sqrt{2}\pi e^{-\sqrt{2}\pi}\,\frac{\sin[2\pi b_c\omega]}{2\pi b_c\omega} + 24\sqrt{2}\pi e^{-2\sqrt{2}\pi}\,\frac{\sin[4\pi b_c\omega]}{4\pi b_c\omega}\right.$$
$$\left. +3\pi^2(13-\sqrt{2}\pi)e^{-\sqrt{2}\pi}\,\frac{\cos[2\pi b_c\omega]}{(2\pi b_c\omega)^2}\right). \tag{3.11}$$

For $d = 6$, we have $\sigma_{\rm geo} = (\pi^2/2)b_c^4$ with $b_c = \sqrt{5/3}r_c$ and $r_c = (5/2)^{1/3}r_h$ as well as $\eta_c = \sqrt{3}$ and the general formula (3.7) then reduces to

$$\sigma_{\rm abs}^{\rm ST\,d=6}(\omega) \approx \sigma_{\rm geo}\left(1 - 16\sqrt{3}\pi e^{-\sqrt{3}\pi}\,\frac{\sin[2\pi b_c\omega]}{2\pi b_c\omega} + 32\sqrt{3}\pi e^{-2\sqrt{3}\pi}\,\frac{\sin[4\pi b_c\omega]}{4\pi b_c\omega}\right.$$
$$\left. +16\pi^2\frac{(-114+5\sqrt{3}\pi)}{15}e^{-\sqrt{3}\pi}\,\frac{\cos[2\pi b_c\omega]}{(2\pi b_c\omega)^2}\right). \tag{3.12}$$

It should be noted that, in (3.11) and (3.12), we have discarded the fifth term of (3.7) which we have found numerically negligible.

3.3. Application 2: The four-dimensional Reissner-Nordtröm black hole

We also apply the general theory developed in subsection 3.1 to the four-dimensional Reissner-Nordtröm black hole (see, e.g., Ref. [11]). In this case, we have

$$f(r) = 1 - \frac{2M}{r} + \frac{Q^2}{r^2} \tag{3.13}$$

where M is the mass of the black hole and Q denotes its charge and we shall assume that $M > Q$. This black hole has inner and outer horizons located respectively at

$$r_- = M - \sqrt{M^2 - Q^2}, \tag{3.14a}$$
$$r_+ = M + \sqrt{M^2 - Q^2}. \tag{3.14b}$$

We are interested only in the outer horizon with radius at $r_h = r_+$ because we have $f(r) > 0$ for $r \in]r_h, +\infty[$. The photon sphere is then located at

$$r_c = \frac{1}{2}(3M + \sqrt{9M^2 - 8Q^2}), \tag{3.15a}$$

(let us note that $r_c > r_h$) and the associated η_c parameter is given by

$$\eta_c = \sqrt{1 - \frac{2Q^2}{r_c^2}}. \tag{3.15b}$$

The critical impact parameter $b_c = r_c/\sqrt{f_c}$ reads

$$b_c = \frac{\sqrt{3}r_c}{\sqrt{1 - Q^2/r_c^2}} \tag{3.15c}$$

and we have for the corresponding geometrical cross section

$$\sigma_{\rm geo} = \pi b_c^2 = \frac{3\pi r_c^2}{1 - Q^2/r_c^2}. \tag{3.15d}$$

For this four-dimensional Reissner-Nordström black hole, the general formula (3.7) then reduces to

$$\begin{aligned}\sigma_{\rm abs}^{\rm RN\,d=4}(\omega) \approx \sigma_{\rm geo} \Bigg\{ & 1 - 8\pi\eta_c e^{-\pi\eta_c} \frac{\sin[2\pi b_c\omega]}{2\pi b_c\omega} + 16\pi\eta_c e^{-2\pi\eta_c} \frac{\sin[4\pi b_c\omega]}{4\pi b_c\omega} \\ & - \frac{4\pi^2 e^{-\pi\eta_c}}{9\eta_c^4} \left[\left(13 - \frac{72Q^2}{r_c^2} + \frac{123Q^4}{r_c^4} - \frac{82Q^6}{r_c^6} \right) \right. \\ & \left. - \frac{\pi\eta_c}{3} \left(7 - \frac{18Q^2}{r_c^2} - \frac{39Q^4}{r_c^4} + \frac{50Q^6}{r_c^6} \right) \right] \frac{\cos[2\pi b_c\omega]}{(2\pi b_c\omega)^2} \Bigg\}. \end{aligned} \tag{3.16}$$

In (3.16), we have discarded the fifth term of (3.7) which we have found numerically negligible.

4. Concluding remarks

The existence of a simple fine structure in the "absorption spectrum" of black holes is an interesting feature which, to our knowledge, has never been noted and which, furthermore, must be certainly pointed out from a theoretical point of view. As was already the case for the fluctuations around the capture cross section of the black hole, this fine structure is only due to the "surface wave" trapped near the photon sphere which is associated with the first Regge pole. However, as emphasized at the end of section 2, for the interpretation of the fine structure, we must now take into account the multiple circumnavigations around the black hole of this surface wave as well as its dispersive character. It is moreover important to recall the duality existing between the Regge poles and the complex frequencies of the weakly damped quasinormal modes of the black hole (see Refs. [12, 13, 14]). It could permit us to provide an interpretation of the fine structure of the high-energy absorption cross section for black holes in terms of quasinormal modes.

For the Schwarzschild black hole, the amplitude of the fine structure is around $5 - 10\,\%$ of that of the eikonal fluctuations, so, in our opinion, its existence could even have interesting physical consequences. This could be the case, for example, in the

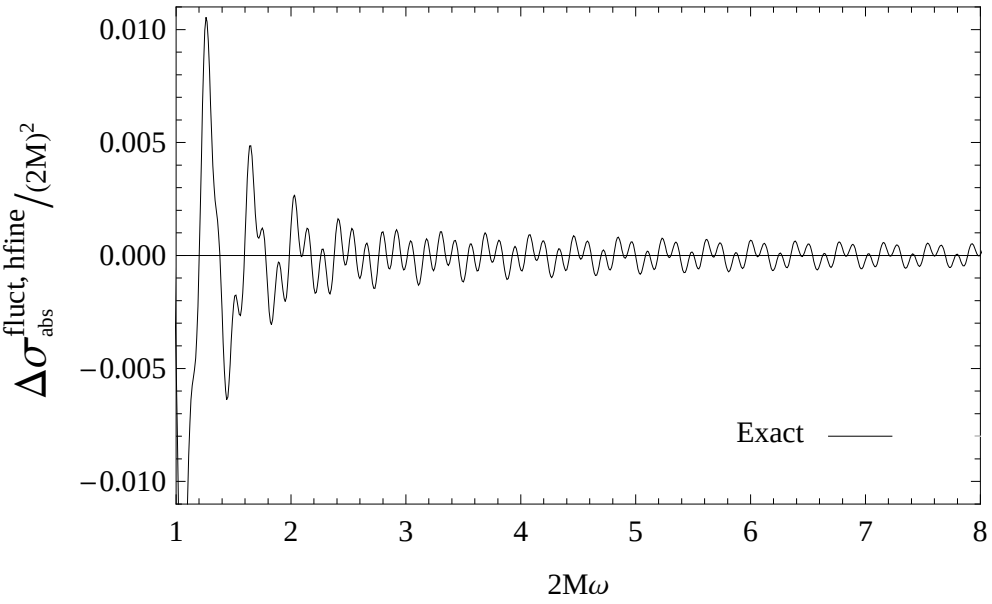

Figure 3. Hyperfine structure of the total absorption cross section for a massless scalar field propagating in the Schwarzschild geometry.

context of strong gravitational lensing. Indeed, as we have already noted in Ref. [13], until now strong gravitational lensing has mainly been considered in the framework of geometrical optics. A description based on wave concepts and, in particular on Regge pole techniques, could furnish a more correct description with new effects predicted. As we have also remarked, the nonlinearities of the Regge trajectories could induce possible observational consequences. Some speculations/results contained in two recent papers [19, 20] seem also to indicate that the resonant and absorption spectra of the Schwarzschild black hole could play a crucial role in the context of strong gravitational lensing and, in particular, that high-energy absorption cross section and strong gravitational lensing are intimately related. In that case, the eikonal and fine structures of the absorption cross section of the Schwarzschild black hole could be observed, perhaps even in the very near future, using the new generation of experimental devices still under development (see, e.g., Ref. [21]) and designed in order to explore the effect of spacetime curvature near the event horizon of the supermassive black hole located at the Galactic Center.

To conclude our paper, we invite the reader to look at figure 3 where we have displayed the "hyperfine structure" of the high-energy absorption cross section of the Schwarzschild black hole. It has been obtained by subtracting to the exact fine structure numerically constructed in section 2 the contributions corresponding to the third and fourth terms of (2.12) as well as the smooth contribution $\pi/(12\sqrt{3}M\omega)^2$ discussed in section 2 of Ref. [1]. Even if the curve displayed is a rather regular one (almost for high frequencies), it presents a much more complicated behavior than the fine structure. We think it could be described analytically by taking into account, in

addition to higher harmonics associated with the first Regge pole [and in particular the ($m = 3$)-term of equation (2.11)] and to the nonlinearities associated with the first Regge pole and its corresponding residue [higher order terms of equations (A.13) and (A.14)], the contribution of the second Regge pole [the ($n = 2$)-term of equation (2.8)]. However, because the amplitude of the hyperfine structure is very weak in comparison with that of the fine structure, it does not seem necessary (or even interesting from the physical point of view) to achieve such a description.

Acknowledgments

It is a pleasure to thank Gilles Esposito-Farèse for his interest in our reggeization program of black hole physics and his enthusiasm during the elaboration of our previous joint work on absorption by black holes.

Appendix

The WKB approach developed a long time ago by Schutz, Will and Iyer [22, 23, 24] (see also Ref. [25] for other related aspects) to determine the weakly damped quasinormal frequencies of black holes proved very efficient in order to construct high-frequency asymptotic expansions for the black hole Regge poles (see our previous works [13, 14]). Here, we shall use and extend it to extract, from the black hole greybody factors, high-frequency asymptotic expansions for the Regge pole residues. We shall first consider the ordinary Schwarzschild black hole and then generalize our study to arbitrary static spherically symmetric black holes endowed with a photon sphere.

Appendix A.1. Regge poles and residues of the greybody factors: the Schwarzschild black hole.

We first consider the case of the four-dimensional Schwarzschild black hole. Even if, in section 2 of this paper, we are only interested in the poles and residues of the greybody factors associated with a scalar field theory, we shall here treat the more general case of a field of spin s with $s = 0, 1 \text{ and } 2$ which satisfies the Regge-Wheeler equation, including therefore, in addition to the scalar field theory ($s = 0$), electromagnetism ($s = 1$) and axial gravitational perturbations ($s = 2$). From a technical point of view, the general case does not present no more difficulties than the scalar field case and our results could be helpful in near future.

The wave equations for the scalar field, for the electromagnetic field, and for the axial gravitational perturbations propagating on the Schwarzschild black hole reduce, after separation of variables, to the Regge-Wheeler equation (2.1) but now, instead of the scalar Regge-Wheeler potential (2.2), we must consider the spin-dependent potential

$$V_\ell(r) = \left(\frac{r-2M}{r}\right)\left[\frac{(\ell+1/2)^2-1/4}{r^2}+\frac{2(1-s^2)M}{r^3}\right] \tag{A.1}$$

and we must furthermore assume that the ordinary angular momentum index $\ell \in \mathbb{N}$ satisfies $\ell \geq s$. For $\omega > 0$ and ℓ given, the partial radial amplitude $\phi_{\omega\ell}(r_*)$ still satisfies the boundary conditions (2.3).

Here, it is important to note that the Regge-Wheeler potential $V_\ell(r_*)$ given by (A.1) behaves as a potential barrier and presents a maximum near the photon sphere of the Schwarzschild black hole located at $r_c = 3M$. Let us denote by $r_0(\ell)$ the position of this maximum expressed in the radial Schwarzschild coordinate and by $(r_*)_0(\ell)$ the corresponding tortoise coordinate. From (A.1) it is easy to obtain

$$r_0(\ell) = 3M \left[1 - \frac{(1-s^2)}{9(\ell+1/2)^2} + \underset{\ell+1/2\to+\infty}{\mathcal{O}}\left(\frac{1}{(\ell+1/2)^4}\right)\right] \tag{A.2}$$

and to show that the peak of the Regge-Wheeler potential is given by

$$V_0(\ell) \equiv \left. V_\ell(r_*)\right|_{r_*=(r_*)_0(\ell)} = \left. V_\ell(r)\right|_{r=r_0(\ell)} \tag{A.3}$$

$$= \frac{(\ell+1/2)^2}{27M^2} + \frac{-3+8(1-s^2)}{324M^2} + \underset{\ell+1/2\to+\infty}{\mathcal{O}}\left(\frac{1}{(\ell+1/2)^2}\right). \tag{A.4}$$

For $\ell \in \mathbb{N}$ and $\omega > 0$ with ω^2 near the peak $V_0(\ell)$ of the Regge-Wheeler potential, we can use, following Iyer, Will and Guinn [23, 24, 25], a third-order WKB approximation for the greybody factors (2.4). We have

$$\Gamma_\ell(\omega) = \frac{1}{1+\exp[2\mathcal{S}_\ell(\omega)]} \tag{A.5}$$

where

$$\begin{aligned}\mathcal{S}_\ell(\omega) = \pi k^{1/2}&\left[\frac{1}{2}z_0^2 + \left(\frac{15}{64}b_3^2 - \frac{3}{16}b_4\right)z_0^4\right.\\ &\left. + \left(\frac{1155}{2048}b_3^4 - \frac{315}{256}b_3^2b_4 + \frac{35}{64}b_3b_5 + \frac{35}{128}b_4^2 - \frac{5}{32}b_6\right)z_0^6\right]\\ +\pi k^{-1/2}&\left[\left(\frac{3}{16}b_4 - \frac{7}{64}b_3^2\right) - \left(\frac{1365}{2048}b_3^4 - \frac{525}{256}b_3^2b_4 + \frac{95}{64}b_3b_5 + \frac{85}{128}b_4^2 - \frac{25}{32}b_6\right)z_0^2\right].\end{aligned} \tag{A.6}$$

Here we use the notations

$$z_0 \equiv z_0(\ell,\omega) = \sqrt{2\,\frac{\omega^2 - V_0(\ell)}{V_0^{(2)}(\ell)}}, \tag{A.7}$$

$$k \equiv k(\ell) = -\frac{1}{2}V_0^{(2)}(\ell), \tag{A.8}$$

$$b_p \equiv b_p(\ell) = \frac{2}{p!}\frac{V_0^{(p)}(\ell)}{V_0^{(2)}(\ell)} \quad \text{for} \quad p > 2, \tag{A.9}$$

with $V_0(\ell)$ defined by (A.3) and

$$V_0^{(p)}(\ell) \equiv \left.\frac{d^p}{dr_*{}^p}V_\ell(r_*)\right|_{r_*=(r_*)_0(\ell)} \quad \text{for} \quad p \geq 2. \tag{A.10}$$

Even if the authors of Refs. [23, 24, 25] have obtained the previous formulas for $\ell \in \mathbb{N}$ and $\omega > 0$, they have moreover shown that their results are helpful in order to obtain third-order WKB approximations for the weakly damped complex quasinormal frequencies of black holes. As we have already remarked in Refs. [13] and [14], these same formulas are very efficient in order to construct high-frequency

asymptotic expansions for the black hole Regge poles and, here, we shall use them to extract, from the black hole greybody factors, high-frequency asymptotic expansions for the Regge pole residues. First, we consider that $\omega > 0$ but we transform the angular momentum ℓ appearing in the previous equations into a complex variable $\lambda = \ell + 1/2$ and we then consider the analytic extension $\Gamma_{\lambda-1/2}(\omega)$ of the greybody factors $\Gamma_\ell(\omega)$ defined by (2.4) and (A.5) as well as the analytic extension $\mathcal{S}_{\lambda-1/2}(\omega)$ of the "phases" $\mathcal{S}_\ell(\omega)$ given by (A.6). The (Regge) poles of the greybody factors are the solutions $\lambda_n(\omega)$ of the equation

$$\mathcal{S}_{\lambda-1/2}(\omega) = i(n-1/2)\pi \quad \text{with} \quad n \in \mathbb{N} \setminus \{0\} \tag{A.11}$$

(here we consider only those of the poles lying in the first quadrant of the complex λ plane) and it is easy to prove that the corresponding residues are given by

$$\gamma_n(\omega) = \frac{-1/2}{\left[d\,\mathcal{S}_{\lambda-1/2}(\omega)/d\lambda\right]\big|_{\lambda=\lambda_n(\omega)}}. \tag{A.12}$$

By inserting (A.2) into (A.6) and considering the transformation $\ell \to \lambda - 1/2$, we obtain from (A.11) the asymptotic expansion

$$\begin{aligned}\lambda_n(\omega) = {} & 3\sqrt{3}\,M\omega + i\,(n-1/2) + \left(\frac{60\,(n-1/2)^2 - 144(1-s^2) + 115}{1296\sqrt{3}}\right)\frac{1}{M\omega} \\ & -i\,(n-1/2)\left(\frac{1220\,(n-1/2)^2 - 6912(1-s^2) + 5555}{419904}\right)\frac{1}{(M\omega)^2} \\ & + \underset{M\omega\to+\infty}{\mathcal{O}}\left(\frac{1}{(M\omega)^3}\right)\end{aligned} \tag{A.13}$$

for the Regge poles (in agreement with the results of Ref. [13]). Finally, from (A.2), (A.6), (A.12) and (A.13), we obtain for the Regge pole residues

$$\begin{aligned}\gamma_n(\omega) = {} & -\frac{1}{2\pi} + i\left(\frac{5(n-1/2)}{108\sqrt{3}\pi}\right)\frac{1}{M\omega} \\ & + \left(\frac{3660\,(n-1/2)^2 - 6912(1-s^2) + 5555}{839808\pi}\right)\frac{1}{(M\omega)^2} + \underset{M\omega\to+\infty}{\mathcal{O}}\left(\frac{1}{(M\omega)^3}\right).\end{aligned} \tag{A.14}$$

It should be noted that, in order to describe the fine structure of the high-energy absorption cross section of the Schwarzschild black hole, we need only the first three terms of (A.13) and the first two terms of (A.14). We have provided one more higher order which could be helpful to describe analytically the hyperfine structure of the high-energy absorption cross section (see our final remark in section 4).

Appendix A.2. Regge poles and residues of the greybody factors: static spherically symmetric black holes

We now focus our attention on the more general case of a static spherically symmetric black hole of arbitrary dimension $d \geq 4$ endowed with a photon sphere which has been considered in section 3. As noted in that section, a scalar field theory defined on such a gravitational background, as the scalar field theory defined on the Schwarzschild black hole, is governed by the Regge-Wheeler equation (2.1) and the boundary conditions (2.3) but, now, the Regge-Wheeler potential is no longer given by (2.2) but by the

much more complicate expression (3.3). However, due to the assumptions listed at the beginning of section 3, the behaviors of (2.2) and (3.3) are quite similar. As a consequence, *mutatis mutandis*, the calculations of subsection A.1 of this appendix can be "easily" generalized.

We first note that the Regge-Wheeler potential $V_\ell(r_*)$ given by (3.3) behaves as a potential barrier and presents a maximum near the photon sphere of the black hole located at $r = r_c$. Let us denote again by $r_0(\ell)$ the position of this maximum expressed in the standard radial coordinate and by $(r_*)_0(\ell)$ the corresponding tortoise coordinate. From (3.3) we can obtain

$$r_0(\ell) = r_c \left[1 + \frac{\delta_c}{[\ell + (d-3)/2]^2} + \underset{\ell+(d-3)/2 \to +\infty}{\mathcal{O}} \left(\frac{1}{[\ell + (d-3)/2]^4} \right) \right] \tag{A.15}$$

with

$$\delta_c = \frac{1}{2}(d-2) f_c \left(\frac{(d-2) f_c + r_c^2 f_c^{(2)}}{2 f_c - r_c^2 f_c^{(2)}} \right) \tag{A.16}$$

which generalizes (A.2) and we can then show that the peak of the Regge-Wheeler potential (3.3) which remains defined by (A.3) is now given by

$$V_0(\ell) = \frac{[\ell + (d-3)/2]^2}{r_c^2/f_c} + \frac{\left[d(d-2) f_c - (d-3)^2 \right]}{4 r_c^2/f_c} + \underset{\ell+(d-3)/2 \to +\infty}{\mathcal{O}} \left(\frac{1}{[\ell + (d-3)/2]^2} \right) \tag{A.17}$$

which generalizes (A.4). In equations (A.16) and (A.17) we have used the notations (3.1) introduced at the beginning of section 3.

We can therefore consider that the WKB approximation (A.5)-(A.6) of subsection A.1 remains valid in the more general case considered here. However, in (A.6) we shall now take into account only the terms of orders 1 and 2 of the WKB approximation, i.e., the terms in $k^{1/2} z_0^2$, $k^{1/2} z_0^4$ and $k^{-1/2}$, in order to avoid heavy calculations and because the description of the fine structure of the absorption cross section can be fully achieved with that precision. Then, by inserting (A.15) into (A.6) and using now the transformation $\ell \to \lambda - (d-3)/2$, we obtain from (A.11) the asymptotic expansion

$$\lambda_n(\omega) = \frac{r_c}{\sqrt{f_c}}\, \omega + i\eta_c (n - 1/2) + \frac{a_n/2}{(r_c/\sqrt{f_c})\omega} + \underset{(r_c/\sqrt{f_c})\omega \to +\infty}{\mathcal{O}} \left(\frac{1}{[(r_c/\sqrt{f_c})\omega]^2} \right) \tag{A.18}$$

with

$$\begin{aligned} a_n = & -\frac{1}{1152 \eta_c^4} \left\{ 288 f_c^2 \left[(d^2 - 2d - 1) f_c - (d-3)^2 \right] \right. \\ & + 144 r_c^2 f_c f_c^{(2)} \left[2(d-3)^2 - (2d^2 - 4d - 3) f_c \right] - 72 r_c^3 f_c^2 f_c^{(3)} \\ & - 18 r_c^4 \left[4(d-3)^2 \left(f_c^{(2)} \right)^2 - 4(d-3)(d+1) f_c \left(f_c^{(2)} \right)^2 + f_c^2 f_c^{(4)} \right] \\ & \left. + 36 r_c^5 f_c f_c^{(2)} f_c^{(3)} + r_c^6 \left[36 \left(f_c^{(2)} \right)^3 - 7 f_c \left(f_c^{(3)} \right)^2 + 9 f_c f_c^{(2)} f_c^{(4)} \right] \right\} \\ & + (n - 1/2)^2 \frac{r_c^3 f_c}{96 \eta_c^4} \left\{ 24 f_c f_c^{(3)} + 6 r_c f_c f_c^{(4)} - 12 r_c^2 f_c^{(2)} f_c^{(3)} + r_c^3 \left[5 \left(f_c^{(3)} \right)^2 - 3 f_c^{(2)} f_c^{(4)} \right] \right\} \end{aligned} \tag{A.19}$$

for the Regge poles (in agreement with our results in Ref. [14]). Here, in order to simplify the results, we have used the notations (3.1) and (3.2) of section 3.

Finally, from (A.15), (A.6), (A.12) and (A.18), we now obtain for the Regge pole residues

$$\gamma_n(\omega) = -\frac{\eta_c}{2\pi} + i\,\frac{(a_c/2\pi)(n-1/2)}{(r_c/\sqrt{f_c})\omega} + \underset{(r_c/\sqrt{f_c})\omega\to+\infty}{\mathcal{O}}\left(\frac{1}{[(r_c/\sqrt{f_c})\omega]^2}\right) \tag{A.20}$$

with

$$a_c = \frac{r_c^3 f_c}{96\eta_c^4}\left\{24 f_c f_c^{(3)} + 6 r_c f_c f_c^{(4)} - 12 r_c^2 f_c^{(2)} f_c^{(3)} + r_c^3\left[5\left(f_c^{(3)}\right)^2 - 3 f_c^{(2)} f_c^{(4)}\right]\right\}. \tag{A.21}$$

References

[1] Décanini Y, Esposito-Farèse G and Folacci A 2011 Universality of high-energy absorption cross sections for black holes *Phys. Rev.* D **83** 044032

[2] Sánchez N 1978 Absorption and emission spectra of a Schwarzschild black hole *Phys. Rev.* D **18** 1030

[3] Harris C M and Kanti P 2003 Hawking radiation from a (4+n)-dimensional black hole: Exact results for the Schwarzschild phase *J. High Energy Phys.* **10** 014

[4] Jung E and Park D K 2004 Effect of scalar mass in the absorption and emission spectra of Schwarzschild black hole *Class. Quantum Grav.* **21** 3717

[5] Jung E and Park D K 2005 Absorption and emission spectra of an higher-dimensional Reissner-Nordström black hole *Nucl. Phys.* B **717** 272

[6] Doran C, Lasenby A, Dolan S and Hinder I 2005 Fermion absorption cross section of a Schwarzschild black hole *Phys. Rev.* D **71** 124020

[7] Grain J, Barrau A and Kanti P 2005 Exact results for evaporating black holes in curvature-squared Lovelock gravity: Gauss-Bonnet greybody factors *Phys. Rev.* D **72** 104016

[8] Crispino L C B, Oliveira E S, and Higuchi A and Matsas G E A 2007 Absorption cross section of electromagnetic waves for Schwarzschild black holes *Phys. Rev.* D **75** 104012

[9] Dolan S R, Oliveira E S and Crispino L C B 2009 Scattering of sound waves by a canonical acoustic hole *Phys. Rev.* D **79** 064014

[10] Crispino L C B, Dolan S R and Oliveira E S 2009 Scattering of massless scalar waves by Reissner-Nordström black holes *Phys. Rev.* D **79** 064022

[11] Misner C W, Thorne K S and Wheeler J A 1973 *Gravitation* (Freeman W H and Company, San Francisco)

[12] Décanini Y, Folacci A and Jensen B P 2003 Complex angular momentum in black hole physics and quasinormal modes *Phys. Rev.* D **67** 124017

[13] Décanini Y and Folacci A 2010 Regge poles of the Schwarzschild black hole: A WKB approach *Phys. Rev.* D **81** 024031

[14] Décanini Y, Folacci A and Raffaelli B 2010 Unstable circular null geodesics of static spherically symmetric black holes, Regge poles, and quasinormal frequencies *Phys. Rev.* D **81** 104039

[15] Cardoso V, Miranda A S, Berti E, Witek H and Zanchin V T 2009 Geodesic stability, Lyapunov exponents, and quasinormal modes *Phys. Rev.* D **79** 064016

[16] Andersson N 1994 Complex angular momenta and the black-hole glory *Class. Quantum Grav.* **11** 3003

[17] Gubser S S 1997 Can the effective string see higher partial waves? *Phys. Rev.* D **56** 4984

[18] Tangherlini F R 1963 Schwarzschild field in n dimensions and the dimensionality of space problem *Nuovo Cim.* **27** 636

[19] Stefanov I Zh, Yazadjiev S S and Gyulchev G G 2010 Connection between black-hole quasinormal modes and lensing in the strong deflection limit *Phys. Rev. Lett.* **104** 251103

[20] Wei S W, Liu Y X and Guo H 2011 Relationship between high-energy absorption cross section and strong gravitational lensing for black hole *Preprint* arXiv:1103.3822 [hep-th]

[21] Eisenhauer F et al 2008 GRAVITY: getting to the event horizon of Sgr A* *Preprint* arXiv:0808.0063 [astro-ph]

[22] Schutz B F and Will C M 1985 Black hole normal modes: A semianalytic approach *Astrophys. J.* **291** L33

[23] Iyer S and Will C M 1987 Black-hole normal modes: A WKB approach. I. Foundations and application of a higher-order WKB analysis of potential-barrier scattering *Phys. Rev.* D **35** 3621

[24] Iyer S 1987 Black-hole normal modes: A WKB approach. II. Schwarzschild black holes *Phys. Rev.* D **35** 3632

[25] Will C M and Guinn J W 1988 Tunneling near the peaks of potential barriers: Consequences of higher-order Wentzel-Kramers-Brillouin corrections *Phys. Rev.* A **37** 3674